Citation
Li, Z. and Chen, W. and Hao, H. 2019. Numerical study of blast mitigation performance of folded structure with foam infill. Structures. 20: pp. 581-593. http://doi.org/10.1016/j.istruc.2019.06.012

Numerical study of blast mitigation performance of folded structure with foam infill

Zhejian Li[1], Wensu Chen[1], Hong Hao[1]*

[1] *Centre for Infrastructural Monitoring and Protection*
School of Civil and Mechanical Engineering, Curtin University, Australia

*corresponding author: hong.hao@curtin.edu.au

Abstract

Blast mitigation capacity of sacrificial cladding with foam filled open-top Truncated Square Pyramid (TSP) is investigated in this study. Quasi-static crushing tests of the TSP foldcore with two different shapes of rigid Polyurethane (PU) foam as infill are carried out. Numerical model of the crushing test is then constructed and validated using the test data. The calibrated models are then used to evaluate blast mitigation performance of sacrificial cladding with the proposed structures as core. Structural response and blast mitigation performance of two proposed foam filled TSP foldcores are compared with the case without foam infill under various blast scenarios. Peak load transmitted to the cladding protected structure during blast loading is set as primary criterion to evaluate the cladding performance, other parameters such as centre displacement and energy absorption are also selected as criteria. Due to the foam-wall interaction effect, foam filled TSP foldcore shows an effect of "1+1>2" under quasi-static crushing. The proposed TSP foldcore with shaped foam infill has superior quasi-static crushing resistance than the summation of stand-alone TSP foldcore and PU foam infill. When subjected to low intensity blast loading, shaped foam filled TSP foldcore shows similar blast mitigation performance to the case without foam infill in terms of the peak transmitted force. However, under high intensity blast loading, the initial peak transmitted force to the protected structure can be greatly reduced by cladding with foam infilled TSP foldcore.

Keywords: Foam filled; folded structure; sacrificial cladding; energy absorption

1. Introduction

In recent years, sandwich structures are becoming popular in the applications of impact attenuation and blast mitigation. Sacrificial cladding, as one of the blast mitigation systems, received lots of attentions in the last decades. It usually consists of a crushable core sandwiched by two skins, and it is placed directly on the surface of the main structure to mitigate blast [1]. Under blast loading, the crushable core of cladding undergoes large deformation with a constant low stress. During the deformation process, it absorbs large amount of energy and reduces the load transmitted to the structure behind the cladding, thus reducing the local damage on protected structure in the event of blast [2]. The crushable cores of sacrificial cladding are often made of low-density cellular structures. Many different topologies of the cladding core were investigated including corrugated [3], polymer and metallic foams [1, 4-6], honeycomb [7-9], auxetic structure [10], tubular [11] and load-self-cancelling cores [12, 13].

In recent studies, folded structures have been used as core of sandwich structures [14, 15]. Origami foldcore is the structure folded from a single un-broken sheet material along the creases without stretching or twisting of the faces. One of the most widely known folded structures, Miura-type origami, was originally proposed for solar panel deployment by Miura [16] and later used as core of sandwich panel. Comparing with conventional honeycomb panel, sandwich panel with Miura-type foldcore has advantages such as continuous manufacturing and open channel design to reduce heat and humidity. However, its crushing resistance is not comparable to honeycomb of the same weight [17]. Another type of folded structure is kirigami folded structure where the sheet material is cut or stamped prior to folding. Many complex geometries can be made by kirigami foldcore, some of which can achieve higher crushing resistance than Miura-type [18].

To further improve the crushing capacity while maintaining loading-rate insensitive behaviour, new form of open-top truncated square pyramid structure (TSP) foldcore has been developed [19]. The inclined sidewalls of TSP are connected via triangular interconnections, which is different from many other kirigami foldcores where sidewalls between unit cells are often not connected. Due to its unique geometries, higher crushing resistance and uniform collapsing with low ratio of peak to average crushing force have been demonstrated over Miura type foldcore and the existing cube strip kirigami foldcore [18, 19]. Under dynamic crushing, the crushing behaviour of the proposed TSP foldcore remains uniform with little increase in peak stress, which is ideal for the applications of energy absorber. The blast mitigation capability of TSP foldcore as sacrificial cladding was studied and compared with conventional honeycomb, Miura-type foldcore and aluminium foam of the same density [20, 21]. Superior performance of TSP foldcore was demonstrated as compared to the other three types of structures.

In this study, the performances of sacrificial claddings with foam filled TSP folded structure as core are investigated. Two shapes of filled foam, i.e. cubic and shaped rigid Polyurethane (PU) foam are considered. The foam infill could provide constraints to the inclined sidewalls of TSP folded structure during the collapsing of the structure, therefore achieving the “1+1>2” effect. In other words, the foam filled TSP foldcore could have higher crushing resistance than the summation of stand-alone TSP foldcore and stand-alone foam block. Quasi-static crushing tests of foam filled TSP foldcore are carried out and the test results are used to calibrate the numerical model. Structural response of the proposed foam filled structure under different blast intensities is then simulated to evaluate its blast mitigation capacities. The responses of foam filled TSP foldcores are compared with non-foam filled TSP foldcore of the same density. Criteria such as peak load transmitted to protected structure, energy absorption and cladding centre displacement are used to evaluate the performance of the claddings with different configurations.

2. Quasi-static crushing tests

2.1 Materials

Rigid PU foam has been widely used as insulation layer or shock absorbing material for transportation packages. Performance of PU foam has been also investigated as cladding for blast loading [4], or infill of sandwich panel against impact loading [22]. PU foam has similar crushing behaviour to aluminium foam which can be divided into three regimes: elastic, plastic and densification [4, 23]. Parameters including plateau stress, σ_0 and densification strain, ε_D are used to define the crushing behaviour of such material. The densification strain, ε_D is the strain where sharp rise of compressive stress occurs due to compacting of the cellular material. It is usually defined by the intersection of two asymptotic lines at plateau and densification regime of a stress-strain curve [24], as shown in Figure 1. Plateau stress, σ_0 is the average crushing stress before densification, and can be defined by the following equation:

$$\sigma_0 = \frac{\int_0^{\varepsilon_D} \sigma(\varepsilon) \cdot d\varepsilon}{\varepsilon_D} \tag{1}$$

where σ is the crushing stress, ε is strain and ε_D is the densification strain.

PU foam used in this study has a density of 35 kg/m^3, named as PU35. Its mechanical properties are measured under quasi-static loading condition (2 mm/min, $\dot{\varepsilon}$=0.00033 s^{-1}) using Lloyd-Ametek EZ50 material testing machine. Cylindrical specimens with diameter of 100 mm and height of 100 mm are prepared for the material compression tests. The stress-strain curve is shown in Figure 1, where both the plateau stress σ_0 and densification strain ε_D are marked.

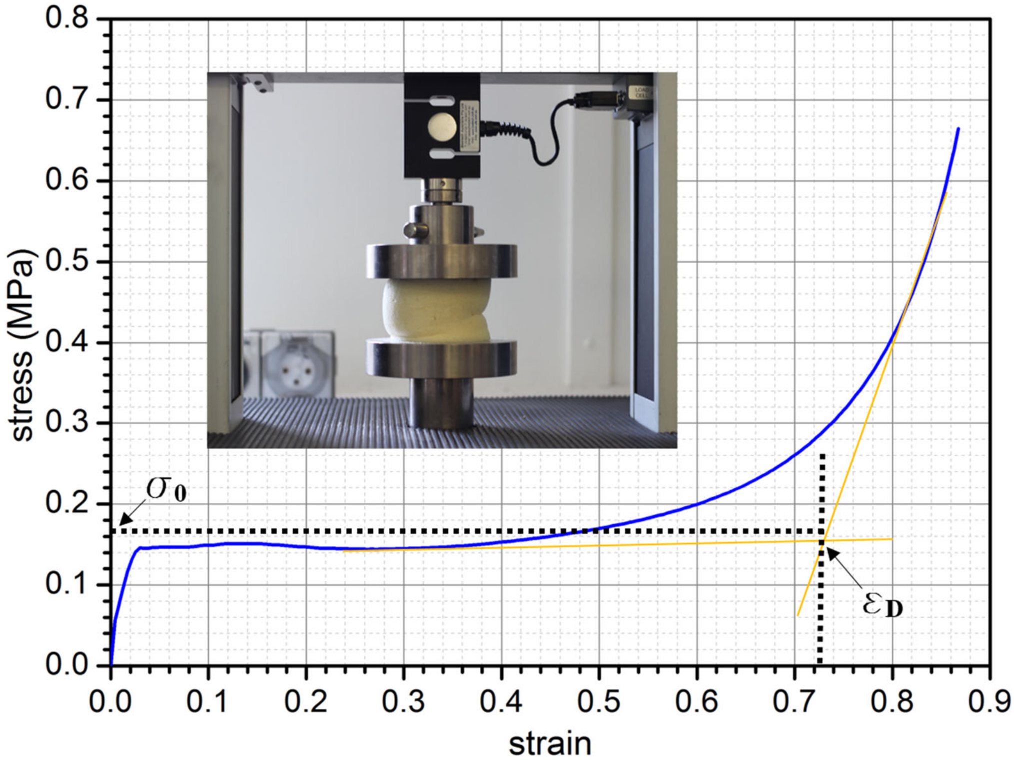

Figure 1. Engineering stress-strain curve of PU35, two yellow lines are the asymptotic lines which determine the densification strain ε_D at their intersection

The TSP foldcores are folded from 1060 aluminium sheet with the thickness of 0.26 ± 0.01 mm. As per the standard ASTM E8M-04 [25], aluminium strip specimens are prepared and tested under quasi-static condition with a constant loading rate of 0.5 mm/min. Two-dimensional digital image correlation (DIC-2D) technique is used to measure the strain and displacement fields of the specimens. DIC strain field of aluminium strip specimen at the maximum strain is shown in Figure 2. The surface strain is retrieved from successive digital images by using the software GOM 2D-DIC. The tensile stress is obtained by dividing the tensile force by the cross-sectional area of the strip. The measured engineering stress-strain data is then converted to the true stress-strain data. Material properties and true stress-strain data are given in Table 1. True stress-strain plot of Aluminium 1060 can be found in the previous study [26].

Table 1. Material properties and true stress-strain data of Aluminium 1060 [26]

Parameter	**Young's Modulus (GPa)**	**Poisson's ratio**	**Yield stress (MPa)**	**Density (kg/m^3)**
Value	69	0.33	67.7	2710

True Strain	0	0.002	0.005	0.013	0.063	0.121
True Stress (MPa)	0	67.7	112.3	120.1	125.8	130.6

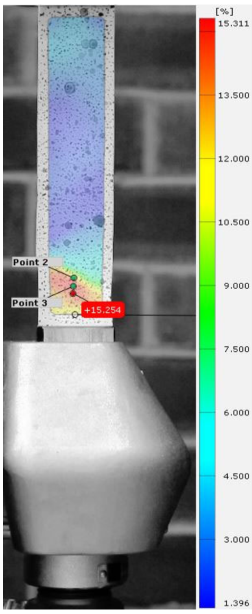

Figure 2. Digital Image Correlation of aluminium strip specimen at the maximum strain [26]

2.2 Test setup

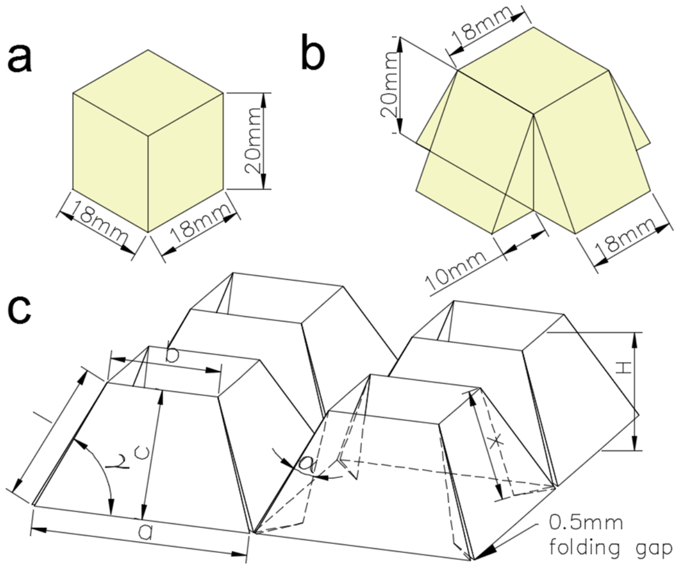

Figure 3. (a) dimension of cubic foam infill; (b) dimension of shaped foam infill; (c) TSP foldcore with four unit cells

A total of five cases are tested in this section including: 1) shaped foam; 2) cubic foam; 3) TSP foldcore; 4) shaped foam filled TSP foldcore; 5) cubic foam filled TSP. The dimensions of single unit cell of shaped and cubic foam are shown in Figure 3 (a, b), respectively. Because the sidewalls are connected via triangle interconnections, as shown in Figure 3 (c), the geometry of TSP foldcore is determined by three parameters only, including the length of bottom edge, a and the length of top edge, b and the foldcore height H. Other parameters can be determined from a, b, and H, as detailed in [20]. The total surface area (A_{surf}) for each TSP unit cell can be expressed as

$$A_{surf} = 4 \cdot \frac{1}{2} c(a+b) + 8 \cdot \frac{1}{2} \sin\alpha \cdot Xl \quad (2)$$

The relative density, or volumetric density (ρ_v) can be calculated by

$$\rho_v = \frac{A_{surf} \cdot T}{a^2 H} \quad (3)$$

where T is the thickness of the sheet.

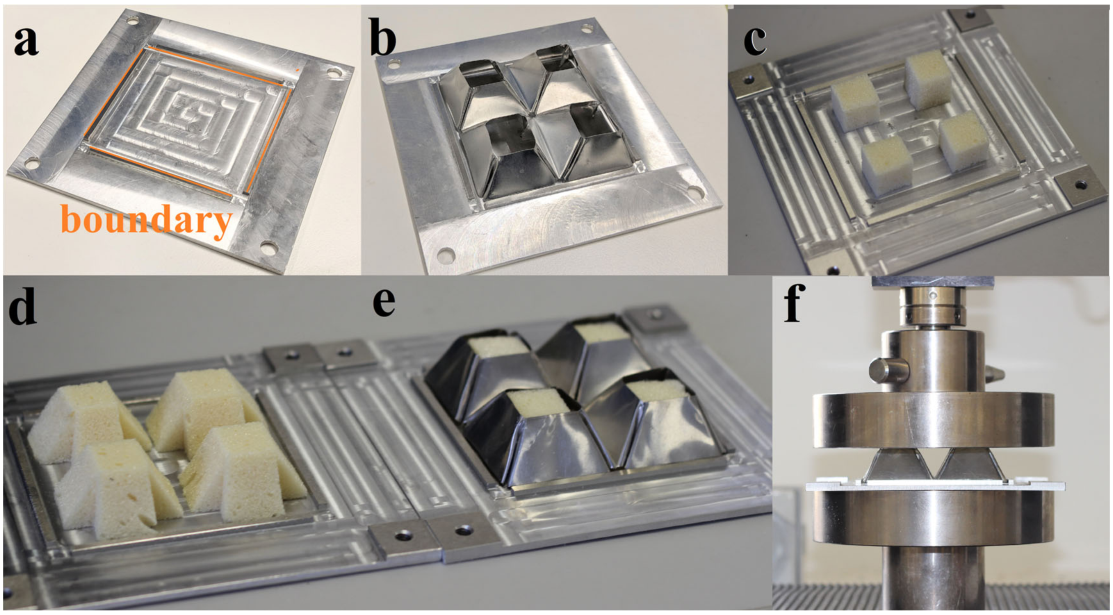

Figure 4. (a) steel base plate with 2 mm high boundary strip; (b) TSP foldcore without foam infill; (c) cubic foam units; (d) shaped foam units; (e) shaped foam filled TSP foldcore; (f) crushing of foldcore specimen

All specimens are crushed under quasi-static loading condition with a constant loading rate of 1mm/min ($\dot{\varepsilon}$=0.00083 s^{-1}) using Lloyd-Ametek EZ50 material testing machine. All specimens have four unit cells and the same height H of 20 mm. Imperfections are inevitable at this stage as all specimens are manually folded. The designed base size of TSP foldcore is 80x80 mm whereas the actual base size of manually folded specimen is around 82x82mm, slightly larger than the designed size. To justify this handcrafting variations, three tests are carried out for each case, and the curve closest to the average is picked for analysis. It is worth noting that the variations between the specimens are little at between 10 to 15%, in terms of average crushing resistance. The foam and foldcore specimens are placed on a steel plate which has 2 mm high boundary strip to constrain the movement of outer bottom edges of the folded structure under lateral crushing. Neither fixing nor glue is applied between the supporting plate and the specimens. Specimens and base plate are shown in Figure 4.

2.3 Crushing tests results

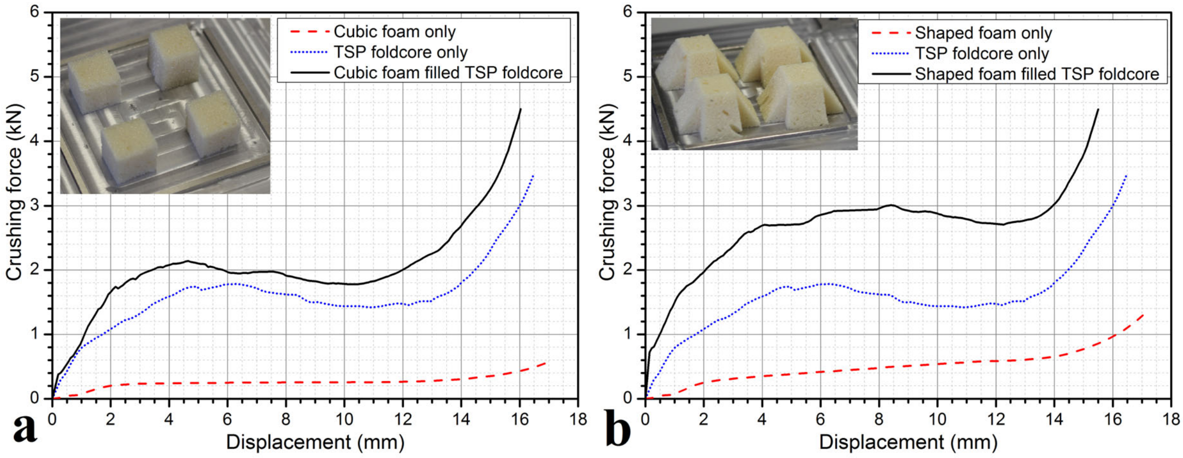

Figure 5. Quasi-static crushing load-displacement curves of (a) cubic foam cases; (b) shaped foam cases

The load-displacement curves of the five cases under quasi-static crushing are shown in Figure 5. The results are divided into two graphs as shown in Figure 5. One includes the cases of cubic foam, TSP foldcore and cubic foam filled foldcore. The other graph includes the cases with shaped foam, TSP foldcore and shaped foam filled foldcore. As shown in Figure 5 (a), the increment of crushing resistance from blue to black lines is slightly larger than the red dash line. In other words, the increase in crushing resistance TSP foldcore with cubic foam infill is larger than the crushing resistance of cubic foam itself. This is more obvious for the case with shaped foam, as shown in Figure 5 (b). The crushing resistance of shaped foam filled foldcore almost doubles that without foam fill. This is consistent with previous studies of foam filled tapered tubes [27, 28].

This can be observed from Table 2 as well, where the average crushing forces of five cases are listed. The average crushing force is calculated from the zero strain to the densification strain, as given in Equation (1). Similar to Figure 1, the densification strain is estimated through the sudden rise in the load-displacement curve. For both cases of foam infills, the enhancements of average crushing resistance are obvious, where the cubic foam filled foldcore has an average crushing force of 1.85 kN slightly greater than 1.49 kN+0.24 kN. Shaped foam filled foldcore has an average crushing force of 2.55 kN, which is 71% higher than TSP foldcore without infill and 33% higher than the sum of the crushing resistance of the two components (1.49 kN+0.43 kN), indicating a “1+1>2” effect.

Table 2. Average crushing forces (**P_{ave}**) of five specimens

	TSP foldcore	**Cubic foam**	**Shaped foam**	**Cubic foam infilled foldcore**	**Shaped foam infilled foldcore**
P_{ave} (kN)	1.49	0.24	0.43	1.85	2.55

This significant increase in crushing resistance of light weight PU foam filled TSP foldcore is caused by the constraint effect to the foldcore sidewalls provided by the foam infill. Similar study of foam or honeycomb filled column had been conducted [29-31]. It was suggested that the cause of increase in crushing resistance of foam filled single column can be divided into two parts, the direct compressive resistance of the foam infill and the constraint or interaction between foam and the column. For a single square column, the interaction between foam and column accounts for 80% of the direct compressive resistance of foam, and this factor is strongly related to the geometry of the column. As given in Table 2, the increment of crushing resistance of cubic foam infill to TSP foldcore is 0.36 kN (1.85-1.49 kN) which is around 1.5 times the compressive resistance of cubic foam (0.24 kN). This means the interaction between cubic foam and foldcore sidewalls accounts for around 50% of the compressive resistance of the cubic foam. The effect of foam-wall interaction is more obvious for the shaped foam filled TSP foldcore, the increment of crushing resistance is 1.06 kN, around 2.47 times of the compressive resistance of shaped foam (0.43 kN), which means the interaction between the shaped foam and sidewalls accounts for 147% of the compressive resistance of the shaped foam. This is because the shaped foam has the same inclined slope as the sidewalls of TSP foldcore. As discussed in the previous study [19], for the TSP foldcore without infill under compressive loading, the top edges of each unit cell tend to bend towards the centre opening, followed by the buckling of the sidewalls,. With the shaped foam infill, the bending of the top edges and buckling of the sidewall become much harder, as the foam infill provides support to the sidewalls from inside each unit cell. Therefore, this foam greatly increases the crushing resistance of TSP foldcore without adding too much weight or alter the crushing behaviour of the TSP foldcore itself. The foam filled TSP foldcores (cubic and shaped) have ideal crushing behaviour to be used as energy absorber with uniform collapsing, low ratio of initial peak to average stress and large densification strain.

3. Numerical simulation for quasi-static loading

3.1 Numerical modelling

Numerical models are constructed to simulate the quasi-static crushing tests of the specimens. The software Solidworks is used for model construction and the finite element software LS-DYNA is used for numerical simulation. The numerical models of two shapes of foam infilled TSP foldcore are shown in Figure 6. The TSP foldcore is constructed using Belytschko-Tsay type shell element and PU foam is modelled using constant stress solid element. The steel base plate with 2 mm boundary strip is also constructed in the numerical model as a rigid plate fixed in all degrees of freedom. As using 1 mm/min in explicit FE analysis could be extremely time-consuming, top rigid block is set to crush the core at a constant rate of 0.5 m/s, instead of 1 mm/min for computational efficiency. The kinetic energy to internal energy ratio of the crushed structure is checked to be less than 5% throughout the crushing and therefore the used crushing speed in numerical simulation is found sufficiently slow to accurately simulate the quasi-static crushing for folded structure. Similar approach was also used in previous studies [17, 18] , in which crushing speed of 2 m/s was used to simulate quasi-static crushing to save computational cost, and satisfactory results were obtained. It should be noted that slower crushing speed substantially increases the computational time. According to the test, crushing process in the numerical simulation terminates at 80% of the structure height, (H=20 mm) which is about 16 mm crushing distance.

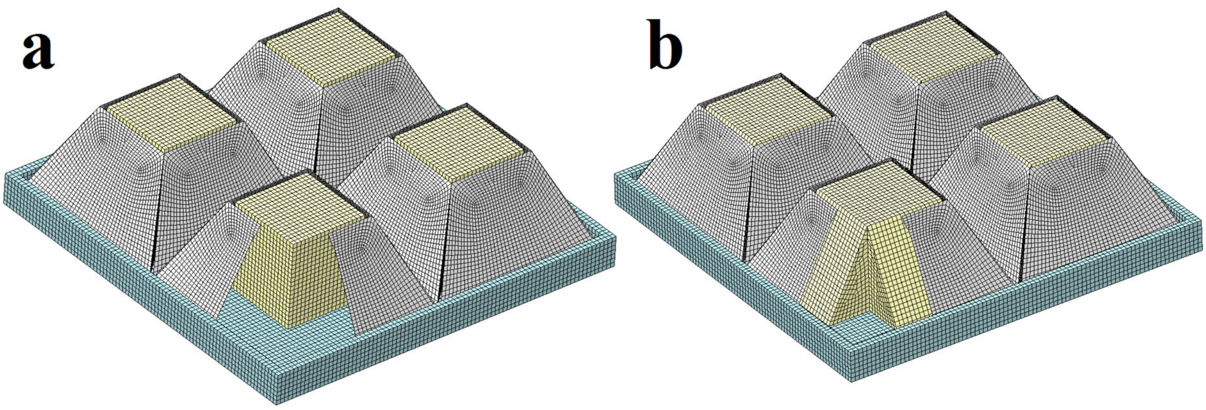

Figure 6. Numerical models of (a) cubic foam filled TSP foldcore; (b) shaped foam filled TSP foldcore, and the rigid base plate with outer boundary. Note a quarter of unit cell has been removed to illustrate the foam infill

The material of PU foam and aluminium sheet are modelled by *MAT063 CRUSHABLE FOAM and *MAT024 PIECEWISE LINEAR PLASTICITY, respectively. The keyword *MAT020 RIGID is used for the top crushing plate and the bottom supporting plate. The material parameters and mechanical properties of PU foam and aluminium sheet are given in Figure 1 and Table 1 of section 2.1. According to the crushing test, no glue nor fixings are presented between any parts in the simulation. For the cases with only foams, the same boundary condition and the same base plate are used in the numerical models. The contacts between TSP foldcore shell elements and top/bottom plates are modelled by the keyword *CONTACT AUTOMATIC NODES TO SURFACE. The keyword *CONTACT AUTOMATIC SURFACE TO SURFACE is used for modelling the contacts between foam and top/bottom plate, foam and TSP foldcore. The keyword *CONTACT AUTOMATIC SINGLE SURFACE is used for self-contact of TSP foldcore. Friction is considered for all contacts with a coefficient of 0.25 [18]. The keyword *CONTACT INTERIOR is used for PU foam to eliminate the issue of negative volume for soft material under large deformation. Mesh convergence test of foam and TSP foldcore had been conducted in previous studies [19, 20], the same element size of 0.5 mm is used for the model in this study. The total number of elements is around 155,000. It takes about 23 hours of CPU time for each case of the quasi-static simulation and around 3 hours for each blast loading simulation. The computer used has the configuration of 8-core Intel Xeon CPU and 32 GB of RAM.

3.2 Model validation

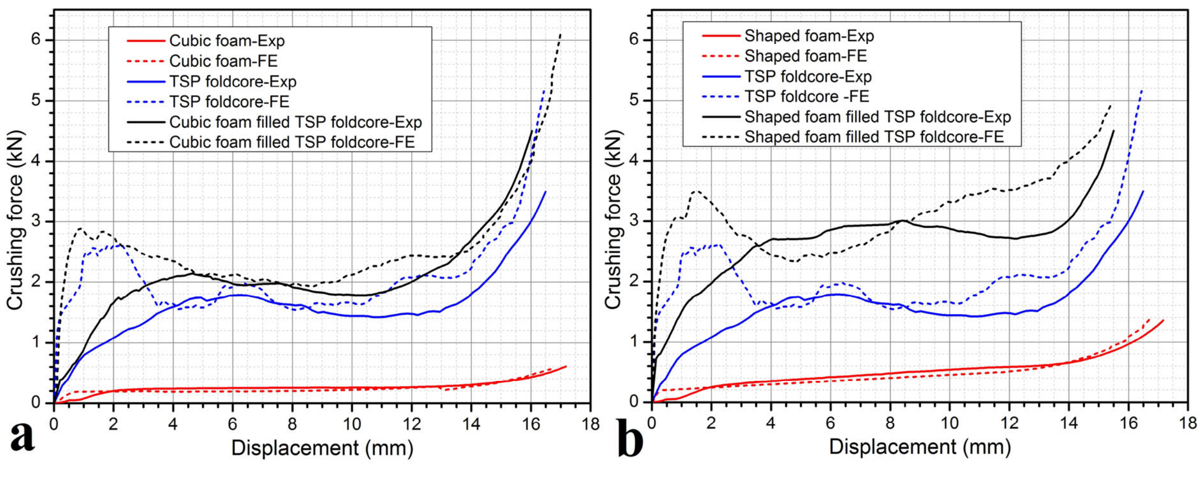

Figure 7. Load-displacement curves of TSP foldcore specimens with (a) cubic foam infill; (b) shaped foam infill, from both experiments (Exp) and FE simulations (FE)

Structural responses of all cases obtained from quasi-static crushing tests and finite element analysis are compared, as shown in Figure 7. The experimental and numerical results including initial peak crushing force, P_{peak}, average crushing force P_{ave}, uniformity ratio, U, and densification strain, ε_D are listed in Table 3. The numerical results including average crushing force and densification strain of all foldcore specimens are in good agreement with the experimental data. However, large discrepancies of initial peak force (P_{peak}) between numerical simulation and tests are shown. This initial differences of crushing resistance are caused by the inevitable imperfection, as all the foldcore specimens were prepared manually. As shown in Figure 4, slight gaps and uneven level of the TSP foldcore unit cell exist. The top surface may not be perfectly at the same level. During the test, the top surface of foam or top edges of TSP foldcore are not perfectly in contact with the top loading plate at the same time. The higher part of the foldcore is in contact with the crushing plate and deforms firstly which led to a smaller initial stiffness of the foldcore and smaller crushing force than FE results. The numerical results matches well with the testing results after the entire core is in contact with the top crushing plate. Similar discrepancy in initial crushing stress between FE and test results has been reported in the hand-folded structure owing to the same reason [18]. A machine pressed Miura-type foldcore using forming dies also showed a lower initial peak stress than FE result [17] owing to imperfect manufacturing.

Table 3. Key parameters from experiments (Exp) and FE simulations (FE)

Specimens		P_{peak} **(kN)**	P_{ave} **(kN)**	**U=** P_{peak}/P_{ave}	ε_D
TSP foldcore	Exp	1.78	1.49	1.19	0.70
	FE	2.59	1.83	1.42	0.71
Cubic foam	Exp	0.20	0.24	0.83	0.75
	FE	0.20	0.21	0.95	0.72
Shaped foam	Exp	0.26	0.43	0.60	0.73
	FE	0.25	0.39	0.64	0.72
Cubic foam filled TSP foldcore	Exp	2.14	1.85	1.16	0.70
	FE	2.89	2.27	1.27	0.71
Shaped foam filled TSP foldcore	Exp	3.01	2.55	1.18	0.71
	FE	3.50	3.04	1.15	0.72

Damage mode of the shaped foam filled TSP foldcore from numerical simulation and test is shown in Figure 8. Similar damage mode can be observed. The sidewalls bend towards the centre of unit cell. The sidewalls on the outer edges of the specimen buckle toward outside of the plate (marked as 1), where some face buckling along the interconnections between sidewalls are presented (marked as 2). The inner faces that connected to other unit cells also buckle toward the centre of unit cell as circled (marked as 3). However, comparing to the numerical results, the damage mode of the crushed specimen from testing is less symmetric and the damage is more randomly distributed.

Overall, the numerical results are in good agreement with the test results as similar values for average crushing force and densification strain are obtained for all cases. The objective of this study is to investigate the effect of foam infill on the blast resistant performance of the TSP foldcore as sacrificial cladding. Due to the perfect geometry of the foldcore in the numerical model, numerical results overestimate the initial stiffness of the structure and thereby overestimate the initial peak stress comparing to the test results. The higher value of initial peak stress leads to a larger peak load transmitted to the protected structure when used as sacrificial cladding under blast loading. Therefore, the numerical model provides a slightly conservative prediction for the foldcore as sacrificial cladding.

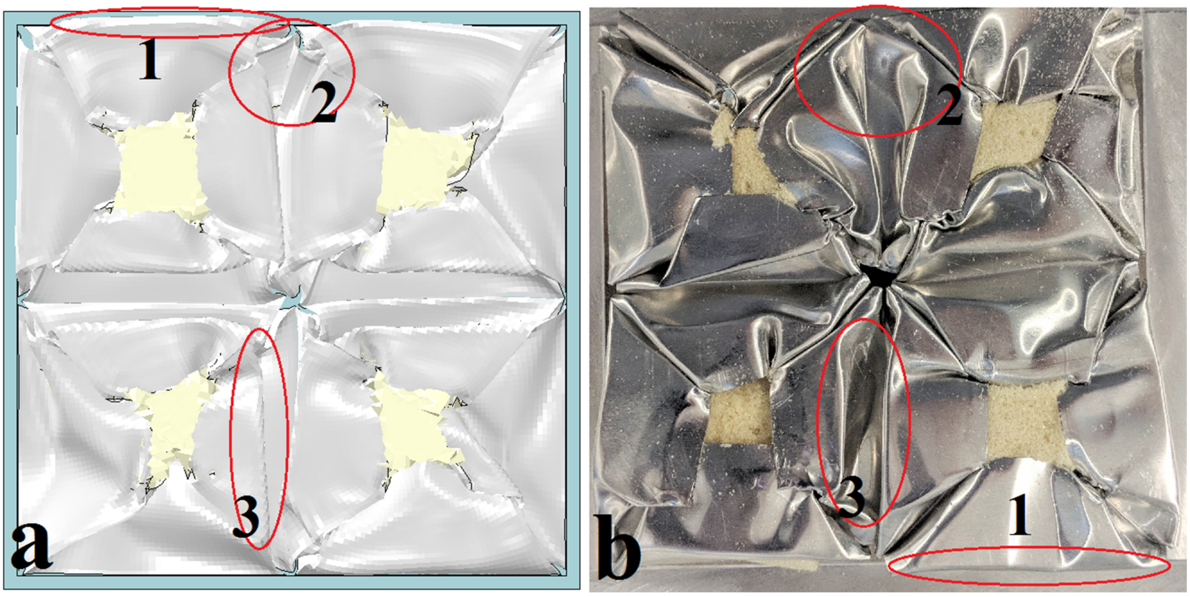

Figure 8. Damage mode of shaped foam filled TSP foldcore (a) FE; (b) experiment

3.3 Damage mode comparison

As shown in the previous sections, the foam filled TSP foldcores demonstrate higher average crushing resistance than the sum of the crushing resistance of two components. The damage modes of three specimens are compared and discussed in this section to explain this observation. Damage modes of TSP foldcores at crushed distance of 10 mm (i.e. 0.5 strain) are shown in Figure 9 (a-c) respectively. For the TSP foldcore without foam infill as shown in Figure 9 (a), the sidewalls around outer boundary bend vertically towards unit cell centre (as circled and marked as 1), other deformations such as corner lift-up and buckling along the intersection of faces can be observed as well. For cubic foam filled foldcore as shown in Figure 9 (b), the damage mode of the foldcore is similar to that without foam. Due to the presence of the foam, the sidewalls experience higher resistance on inward bending, resulting in a slight increase in the lateral crushing resistance of the cubic foam infilled foldcore.

With the shaped foam infill, the damage mode is quite different from the other two cases. In the numerical results as shown in Figure 9 (c), some sidewalls on the outer edges are no longer bending vertically towards centre. For instance, the right side of the sidewalls in Figure 9 (c) bends horizontally near the middle plane towards the outer boundary, while the top edge of these sidewalls rolls towards centre of each unit cell (as circled and marked as 2). This is because the sidewalls of the foldcore and the shaped foam have the same inclined angle. Under lateral crushing, the inward vertical bending (marked as 1) of TSP foldcore sidewalls is much harder to occur due to resistance from the shaped foam. With the bottom edges of foldcore sidewalls constrained by strips on base plate, the sidewalls bend horizontally at middle height. The insertion of shaped foam greatly increases the crushing resistance of the TSP foldcore. It provides extra support to the sidewalls of TSP foldcore under lateral crushing which greatly increases the force required for the sidewalls to deform towards centre of unit cell. In the quasi-static crushing tests, similar change of deformation mode can be observed from inward vertical bending (marked as 1) for foldcore without foam to horizontal bending (marked as 2) for shaped foam filled foldcore, as shown in Figure 9 (d) & (e).

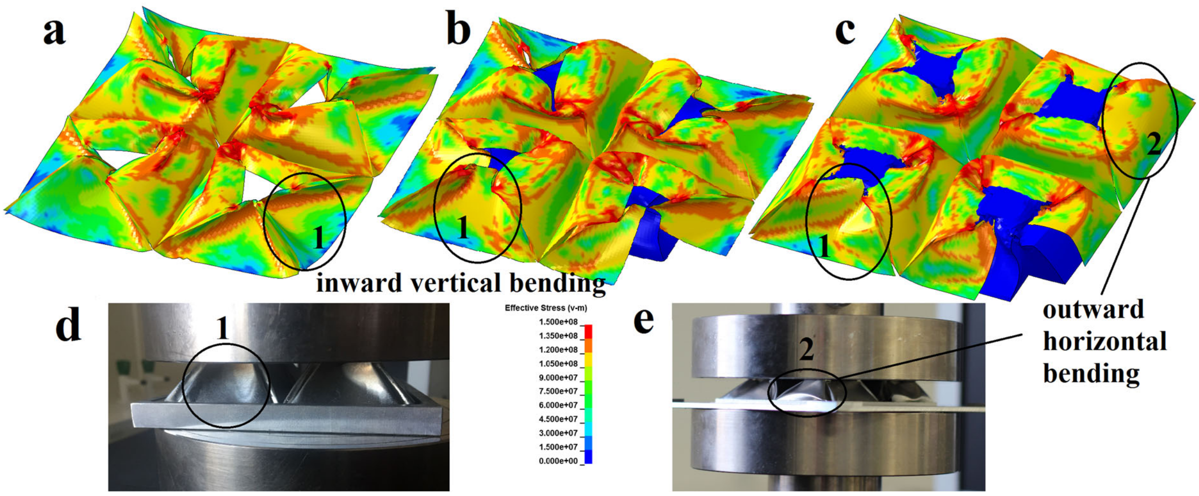

Figure 9. Damage modes of specimens at 10 mm crushed distance (i.e. strain of 0.5) (a) FE results of TSP foldcore; (b) FE results of cubic foam filled foldcore; (c) FE results of shaped foam filled foldcore (d) crushing test of TSP foldcore without foam infill; (e) crushing test of shaped foam filled TSP foldcore; Note: d and e are not at the same crushed distance

4. Blast mitigation capability of foam infilled TSP foldcore

4.1 Sacrificial cladding set up

As previously studied, sacrificial cladding with TSP foldcore as core outperforms conventional honeycomb, Miura-type foldcore and aluminium foam of the same density in terms of blast mitigation capability [20, 21]. This finite element analysis study is aimed to evaluate blast mitigation capability of foam filled TSP foldcore. Four cladding configurations are considered, including: no cladding, TSP foldcore without foam infill, cubic foam filled TSP foldcore and shaped foam filled TSP foldcore. The dimensions of unit cell of the TSP foldcore including the foam infill are scaled up twice with respect to the quasi-static case to have a more practical height of 40 mm as sacrificial cladding. The dimension of TSP foldcore unit cell is scaled from 40 x 40 x 20 mm in the previous sections to 80 x 80 x 40 mm for the blast cladding simulation in this section. The same boundary conditions are applied for the cladding simulation. No glue nor fixing is applied between the front plate, core and the base plate. The base plate is set as rigid plate with a 2 mm-high boundary around the outer edges of the base plate to constrain the in-plane movement of the foldcore sidewalls.

Table 4. Mass distribution of four cladding core configurations with average core density of 100 kg/m^3

Parameter	TSP foldcore	Cubic foam filled TSP foldcore	Shaped foam filled TSP foldcore
Wall thickness (mm)	0.708	0.658	0.604
Mass of foam (g)	-	7.3	15.1
Mass of foldcore (g)	102.4	95.1	87.3
Average core density (kg/m^3)	100	100	100

In the numerical model, mechanical properties for both PU foam and aluminium remain the same as listed above. The densities and overall masses of three foldcore configurations are kept the same by varying the wall thickness of TSP foldcore. Masses of these cladding cores are listed in Table 4, where the average core density of the core is kept the same as 100 kg/m^3. This density is approximately equal to 3.7% relative density of aluminium foam, which is a common material used as core of sacrificial cladding [2, 5, 32]. However, this density of 3.7% used in the study is lower than that of aluminium foam which has the minimum relative density of 5% available on the market [33]. The top skin of the cladding made of aluminium 1060 is set as 160 x 160 x 5 mm for all four cladding configurations. The front plate is constructed with solid element in LS-DYNA. It is worth noting that Aluminium has an insignificant strain rate effect

[34], and the PU foam also has low strain-rate sensitivity especially under higher strain rate (e.g. 2000 s^{-1}) [35]. Therefore, the strain rate effect is not considered in the numerical analysis.

The keyword *LOAD BLAST ENHANCED is used to generate blast loading in LS-DYNA. Different blast intensities are considered in this study by varying explosive weight. The stand-off distance is set to be 1500 mm above the centre of the cladding front plate which is in accordance with the previous field-testing for sacrificial claddings [3, 5]. For the structure without sacrificial cladding, the stand-off distance is 1545 mm, as the cladding has a height of 40 mm plus the 5 mm-thick front plate.

4.2 Structural response

4.2.1 Transmitted force

Table 5. Peak transmitted force, peak crushed distance at centre and energy absorption by parts of different cladding configurations under various blast intensities

Cladding types		P_{peak} (kN)	Peak crushed distance at centre δ (mm)	Energy absorption (J)	
				by TSP foldcore	by foam
1 kg TNT 1.5 m/kg^(1/3)	No cladding	34.3	-	-	-
	TSP foldcore	33.9	1.6	37	-
	Cubic foam filled	25.7	2.3	35	2
	Shaped foam filled	32.3	2.7	40	3
2 kg TNT 1.19 m/kg^(1/3)	No cladding	67.1	-	-	-
	TSP foldcore	38.5	9.1	147	-
	Cubic foam filled	35.0	9.2	141	8
	Shaped foam filled	37.7	10.0	148	15
4 kg TNT 0.95 m/kg^(1/3)	No cladding	132.1	-	-	-
	TSP foldcore	39.2	22.2	567	-
	Cubic foam filled	36.0	24.5	555	25
	Shaped foam filled	31.4	27.8	540	65

The blast intensities of 1, 2 and 4kg of TNT explosion are considered. The time history curves of transmitted force to the base structure with different cladding configurations are shown in Figure 10-12. Other parameters are given in Table 5. The transmitted load-time history curves are obtained from FE result by plotting the reaction forces exerted on base plate of structure. The purpose of using sacrificial cladding is to mitigate blast pressure and reduce the force transmitted to the protected structure. Under blast loading, the front plate moves toward the protected structure and crushes the core of sacrificial cladding. The crushing strength of cladding core is usually much lower than the peak blast pressure, thus reduces the force transmitted during the deformation of the core. Hence, these time-history curves of transmitted force to base structure are used to evaluate the performances and the peak transmitted load to protected structure is selected as the main criterion for the evaluation.

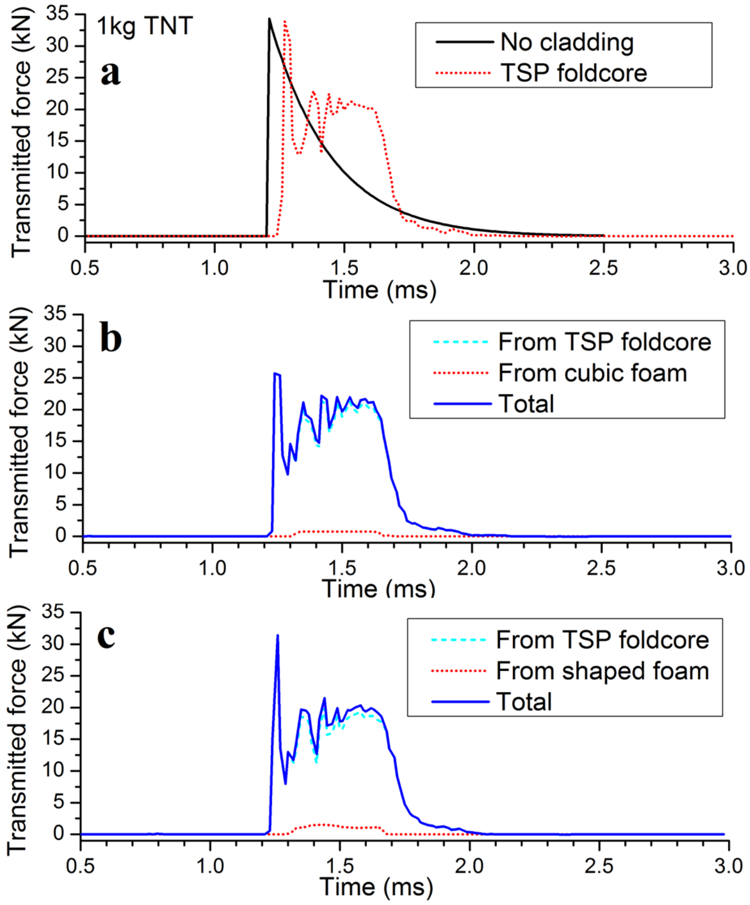

Figure 10. Computed time-history of transmitted forces to protected structure under 1kg TNT explosion at 1.5 m stand-off distance of four cladding configurations (a) no cladding and TSP foldcore without foam infill; (b) cubic foam filled TSP foldcore; (c) shaped foam filled TSP foldcore

As can be seen in Figure 10, the peak value of force transmitted to the base structure from TSP foldcore is similar to the case without cladding under 1 kg TNT explosion weight. By using two types of foam filled TSP foldcores as cladding, the peak transmitted force slightly reduces, while the peak crushed distance at panel centre increases slightly. Similar responses can be observed for these three cladding configurations (TSP foldcore, cubic and shaped foam filled TSP foldcores). The transmitted force history curves start with an initial peak and sudden reduction, followed by a more consistent plateau stage and gradual reduction to zero.

The results shown in Figure 10 indicate that the three types of TSP foldcores have insignificant mitigation capability on the protected structure under this blast intensity, which is too low for cladding to effectively mitigate shock waves. As previously studied [20, 32], each cladding system is only effective under certain blast scenarios. For the case of 1 kg TNT explosion at 1.5 m stand-off distance considered here, these cladding cores have very little deformation due to the low blast pressure comparing to the collapsing stress of the cladding core. Limited energy is absorbed in this process, thus resulting in a less effective blast mitigation performance of these claddings.

The time-history curves of the transmitted force under 2 kg TNT explosion are shown in Figure 11. Comparing to the unprotected structure, the peak transmitted force is reduced by 42.6%, 47.8% and 45.8% for TSP foldcore without foam infill, cubic and shaped foam filled TSP foldcores, respectively. Similar to the 1kg TNT explosion, the peak transmitted force of TSP foldcore is slightly higher than that of the shaped foam filled TSP, followed by the cubic foam filled TSP. However, during the later stage of crushing, slight rise in transmitted force can be observed for the shaped foam filled TSP foldcore between 1.5 and 2 ms (Figure 11 c), which indicates the increase of crushing resistance due to the compacting of the foam at the later stage of deformation. Very little increase can be observed from the cubic foam filled cladding (Figure 11 b) and the cladding without foam infill (Figure 11 a) from 1.5 to 2 ms.

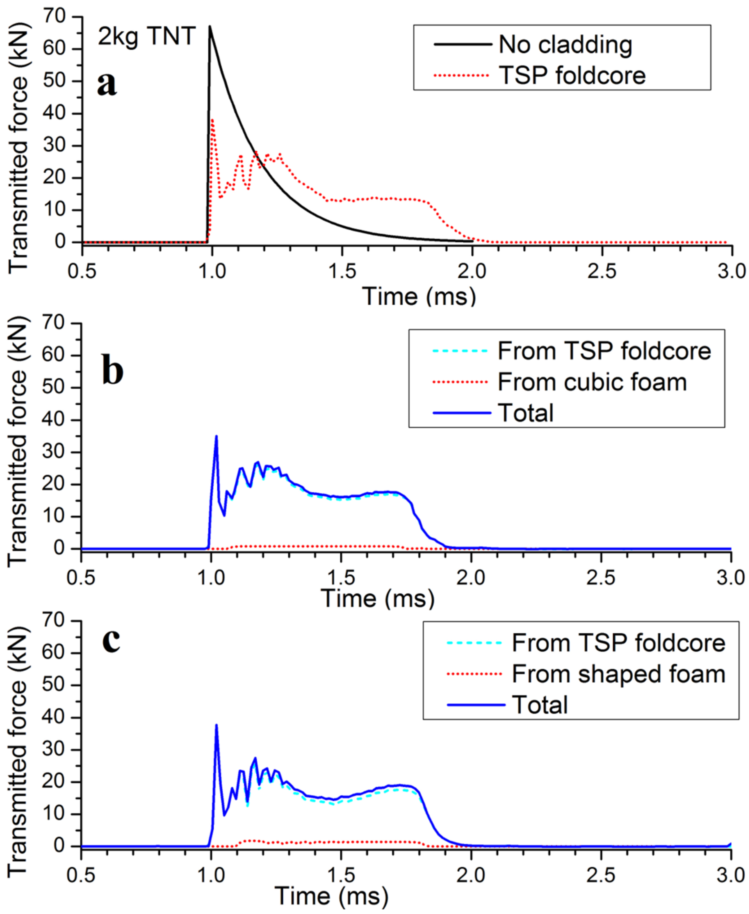

Figure 11. Computed time-history of transmitted forces to protected structure under 2kg TNT explosion at 1.5m stand-off distance of four cladding configurations (a) no cladding and TSP foldcore without foam infill; (b) cubic foam filled TSP foldcore; (c) shaped foam filled TSP foldcore

The results from the scenario of 4kg TNT explosion is shown in Figure 12. Compared to the case of unprotected structure, the peak transmitted force is reduced by 70.3%, 72.7% and 74.8% using TSP foldcore cladding without foam infill, cubic and shaped foam filled TSP foldcores as cladding, respectively. Good blast mitigation capabilities are demonstrated for all the three cladding configurations. The peak transmitted force to protected structure remains similar in value with the increasing blast intensities (1, 2 and 4kg TNT) as shown in Figure 10-12. Low uniformity ratio, which is the ratio between peak force and average force, is also shown for all three cladding configurations. It is worth noting that loading duration under 4 kg TNT explosion is not the same for these three claddings. The foam filled TSP foldcore shows longer loading duration starting from 0.8 ms to 2.1 ms (Figure 12 b&c). For the foldcore without foam infill, the loading finishes at around 1.9 ms, which leads to slightly less energy absorption.

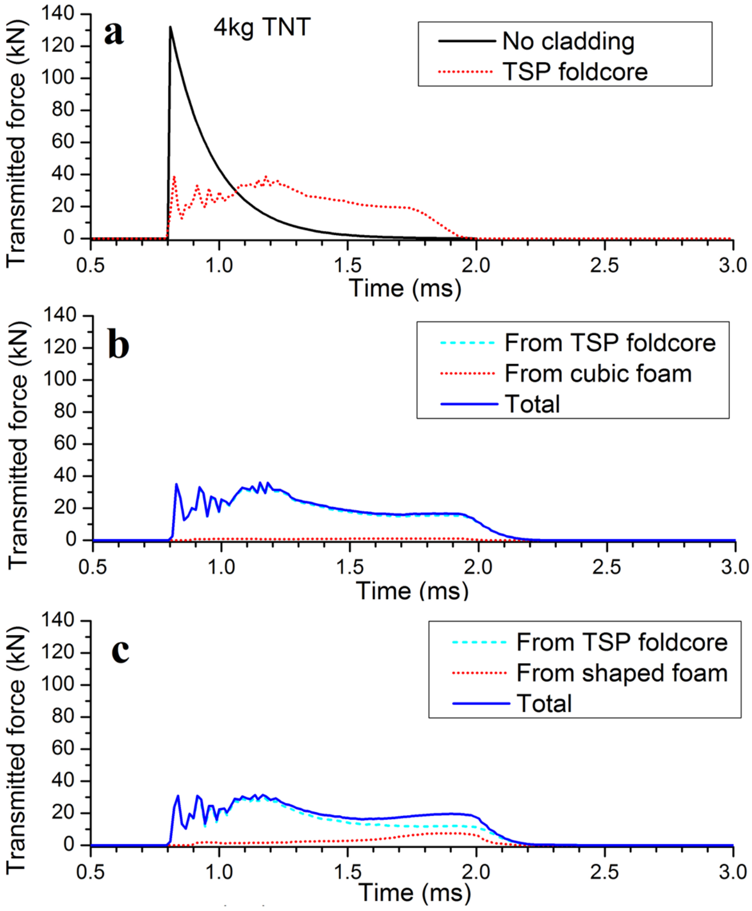

Figure 12. Computed time-history of transmitted forces to protected structure under 4kg TNT explosion at 1.5m stand-off distance of four cladding configurations (a) no cladding and TSP foldcore without foam infill; (b) cubic foam filled TSP foldcore; (c) shaped foam filled TSP foldcore

As previously studied, TSP foldcore without foam infill demonstrated superior blast mitigation capability over conventional square honeycomb and aluminium foam of the same weight [20]. The performances of foam filled TSP foldcore, however, show no significant difference with the non-foam filled case. The foam filled TSP foldcores including cubic and shaped foams have a lower peak transmitted force but a slightly larger peak crushed distance compared to the TSP foldcore without foam infill of the same mass. This indicates that under blast loading, the cubic and shaped foam infilled TSP foldcores are slightly easier to deform as compared with the TSP foldcore without infill which has slightly thicker walls (i.e. 0.708 mm). This slightly lower value of initial peak transmitted force of foam filled TSP foldcore is caused by the difference in wall thickness, as given in Table 4. The initial peak force of TSP foldcore is strongly correlated to the thickness of the vertical triangular interconnections between sidewalls. It was found that the initial peak crushing force of honeycomb structure had a power relationship with the wall thickness [36]. Slight increase in wall thickness may lead to a significant increase in initial peak force for these cellular structures with vertical faces, such as this TSP foldcore.

It can be concluded that the shaped and cubic foam infilled foldcores have slightly better performance in mitigating the peak blast loading transmitted to protected structure than the foldcore without any foam infill when the blast intensities are sufficiently large. The foam filled TSP foldcore can further reduce the peak force transmitted to the protected structure, and the peak centre crushed distance is larger as compared to the case without foam infill, implying more energy dissipation. However, when the blast intensities are small, the blast mitigation performance of three foldcores (TSP foldcore, cubic and shaped foam filled TSP foldcores) are similar in terms of peak transmitted force to the protected structure. As mentioned previously, this is because of limited plastic deformation of the cladding core under low intensity of explosion. It is also worth mentioning that due to the conservation of momentum, the duration of the loading transferring to protected structure is proportional to the reduction in peak stress level, and the impulse transmitted is not necessarily reduced. The global response of the structure may not be affected with this added sacrificial cladding. The sacrificial cladding act as a local protective structure to mitigate local damage caused by the high peak pressure. Similar results have been observed in the previous studies of aluminium foam and PU foam as sacrificial cladding for structure [2, 4].

4.2.2 Damage mode

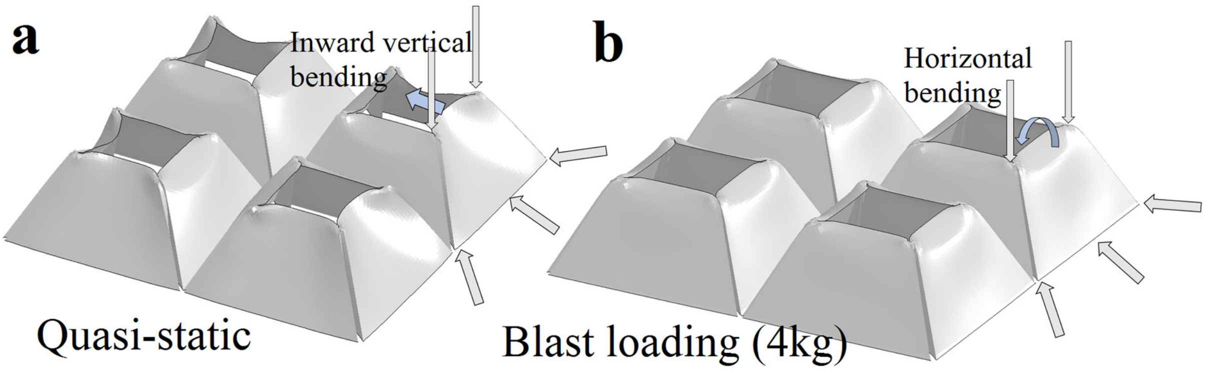

Figure 13. Comparison of computed damage mode of TSP foldcore without foam under (a) Quasi-static crushing; (b) Blast loading of 4 kg TNT explosion

The damage modes of these TSP foldcores with three foam configurations are very different from those under quasi-static loading. The comparison of computed deformation of TSP foldcore without foam under two different loading conditions is shown in Figure 13. The inward vertical bending of the sidewall under quasi-static loading changes to the top edge horizontal bending of the sidewalls under dynamic loading. This change in deformation mode is caused by the inertia effect and the inertial stabilization effect of the lower part of the sidewall under higher crushing speed, as explained in the previous study [26]. As shown in section 3.3, under quasi-static loading, the damage modes are different for all three configurations of the foldcores, resulting in different crushing resistances among the three foldcores. However, under blast loading with 1, 2 and 4 kg TNT blast scenarios, the performances of these claddings including peak transmitted force and energy absorption are similar owing to the similar damage mode under dynamic loading.

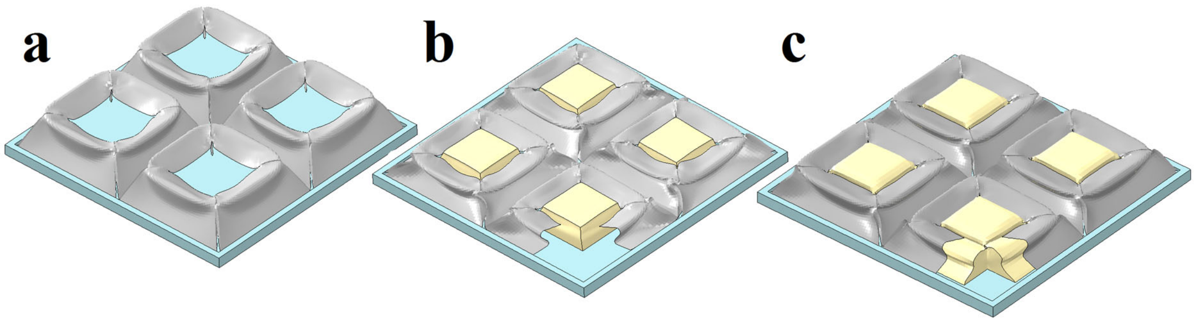

Figure 14. Cladding core computed deformation of (a) TSP foldcore; (b) cubic foam filled; (c) shaped foam filled, at the maximum displacement under 4 kg TNT explosion at 1.5m stand-off distance; Note the front plate is removed for illustration

The computed damage modes of three cladding configurations, i.e., TSP foldcore, cubic foam filled and shaped foam filled TSP foldcore are shown in Figure 14. The vertical mid-plane cross-section views at early and later stages during deformation under both loading conditions are shown in Figure 15. Similar change of deformation mode of TSP foldcore without foam infill was observed as in the previous study [26] under different loading rates. As shown in the figure, the deformation modes under blast loading are almost identical for the three foldcore configurations despite different foam geometries. The top edges of the TSP foldcore bend towards centre opening, and the sidewalls buckle along the horizontal middle line of each sidewall face which is different from the quasi-static damage mode shown in Figure 9 and Figure 15 (a, c). The cubic foam is not in contact with sidewall and provides no support to the foldcore at the early stage of deformation, as can be seen in Figure 15 (b). Under quasi-static loading, the shaped foam is in full contact with the sidewalls of TSP foldcore and provides support to the sidewalls since the starting of the deformation as shown in Figure 15(c, e). This is caused by the inward vertical bending of the sidewalls. However, under dynamic loading, the deformation is more locally distributed along the top edges of the sidewalls therefore resulting in only partial contact to the foam, as in Figure 15 (d, f). Due to the change of deformation mode of the sidewalls under dynamic loading, shaped foam only provides support to sidewalls at the later stage of the deformation when sidewalls buckle and are in full contact with the foam infill, as shown in Figure 15 (c, d). Similarly, under lower blast intensities where the deformation is small and the sidewalls are not in full contact with the foam, the foam infill provides little support to the sidewalls and thus leads to less effectiveness of the foam infill.

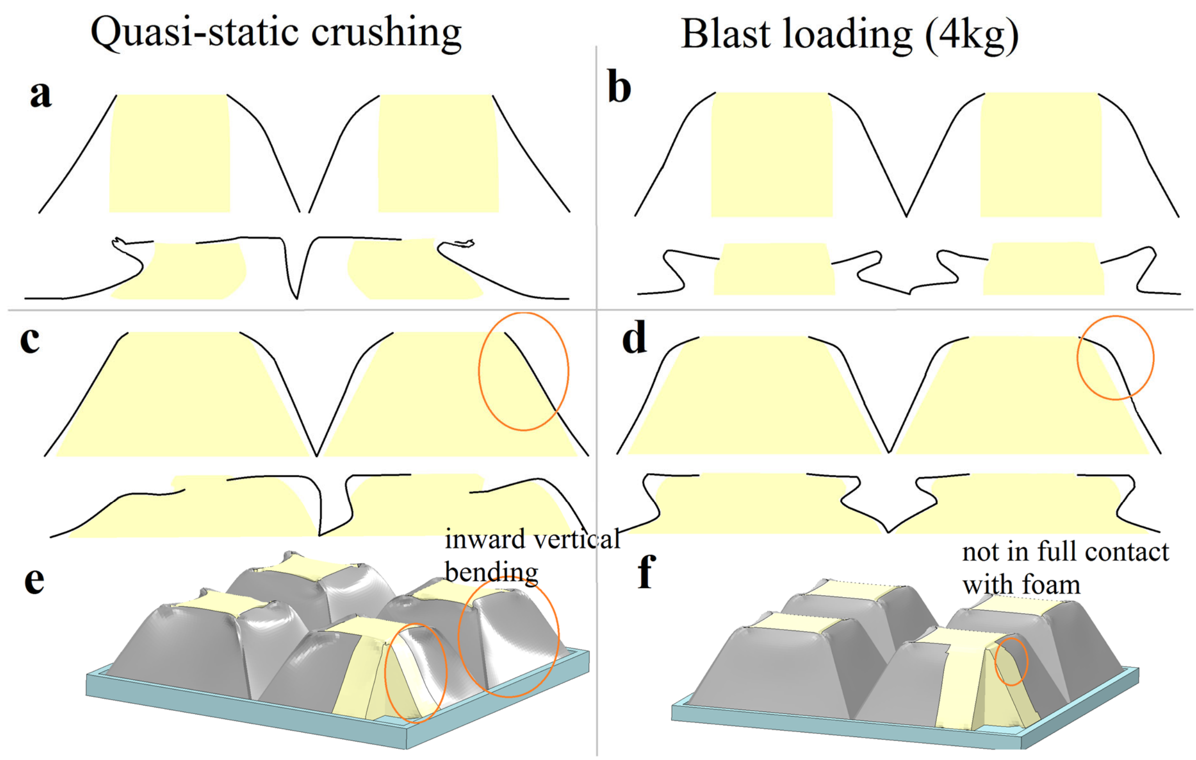

Figure 15. Mid plane cross-section view of the TSP foldcores with (a, b) cubic and (c, d) shaped foam infill at the early and later stages of computed deformation under two loading conditions; (e, f) damage modes of shaped foam filled TSP foldcore at the early stage under two loading conditions

This can also be confirmed in the transmitted force time-history curves as shown in Figure 11 and Figure 12, where the shaped foam infilled TSP foldcore shows higher transmitted force than the other two configurations at the later stage of the loading, i.e. from 1.5 to 2.0 ms. This is when the foldcore sidewalls buckled and come in full contact with the shaped foam which provides extra support at later stage of the deformation. Therefore, the noticeable difference in initial peak force is mostly caused by the wall thickness of the TSP foldcores rather than by the foam infills.

4.2.3 Energy absorption

Specific energy absorption (SEA) of the components including the TSP foldcore and the foam infills are shown in Figure 16 for three cladding configurations and blast intensities. Significant increase of SEA along with the increasing blast load can be observed for all components of three cladding cases. It can be found that the TSP foldcore has a higher SEA than the foam infill under any blast intensity. This is due to the material difference between PU foam and aluminium.

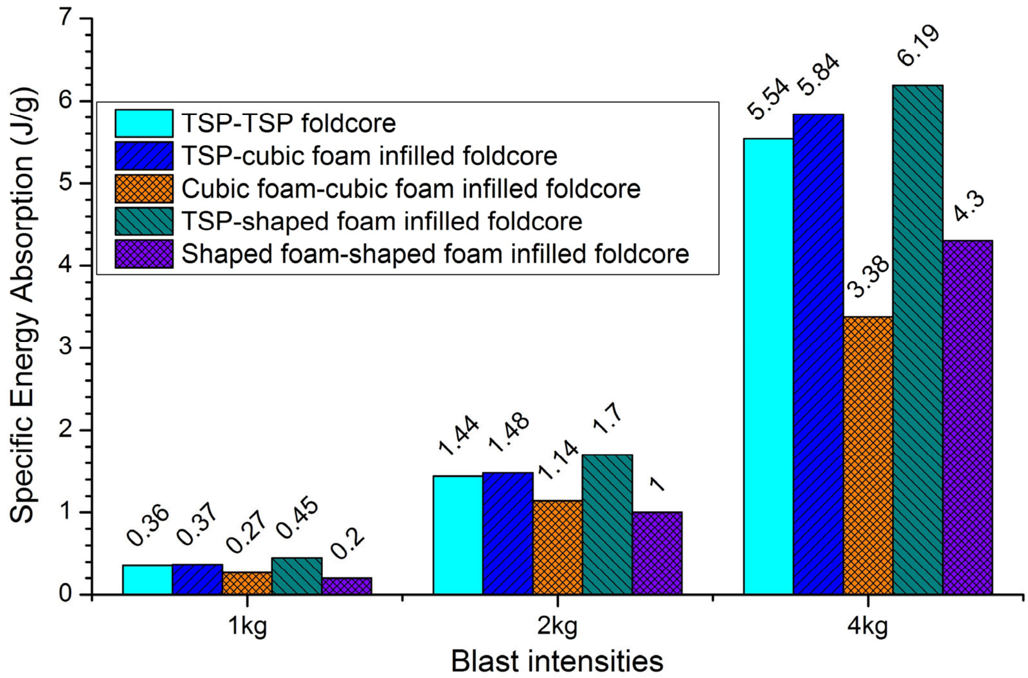

Figure 16. Specific energy absorption (SEA) of different parts of three cladding configurations under different blast intensities

The SEA of shaped foam is lower than that of cubic foam under 1, 2 kg TNT explosion, and higher than that of cubic foam under 4 kg TNT explosion. This can be explained by the geometry of the foam infill. Under lower blast intensity, only the top part of shaped foam deforms during the process and the sidewalls are not in full contact with the foam, therefore foam provides little support to the sidewalls as shown in the previous section. With higher blast intensity, the larger portion of the shaped foam is deformed. Because of its increasing cross-section area from top to bottom, higher crushing resistance of shaped foam at the later stage of the deformation can be observed as shown in Figure 12. Furthermore, the SEA of TSP foldcore increases as well when the shaped foam is inserted. Due to the buckling of the sidewalls at the later stage of the deformation, extra support is provided to the foldcore sidewalls by the shaped foam, which increases the crushing resistance of the TSP foldcore at the later stage. Therefore, SEA of shaped foam filled foldcore is higher than that of the other two cases under intensive blast load, where larger deformation occurs.

4.3 Influence of density

In this section, claddings with average core density of 150 kg/m^3 are simulated under 7kg TNT explosion at 1.5m stand-off distance. This is to match the minimum density of one of the most common cladding core materials, i.e. 150 kg/m^3 aluminium foam with 5% relative density [33]. Furthermore, as mentioned in the previous section, the initial peak crushing force is in power relationship with wall thickness for cellular structures. The effect of wall thickness of the TSP foldcore on the initial peak force is greatly reduced with higher average core density of the core, and the effect of foam infill is more obvious. Given the overall core density of 100 kg/m^3 same as the previous section, the wall thickness of TSP foldcore has a difference of 17.2% between the cladding without foam and the cladding with shaped foam infill. This difference reduces to 8.9% for the core density of 150 kg/m^3. Only overall core density and the blast loading are changed in this section, other parameters and boundary conditions are kept the same as in the previous sections. The configurations of three cladding cores are given in

Table *6*.

Table 6. Mass distribution of three cladding core configurations with average core density of 150 kg/m^3

Configuration	**TSP foldcore**	**Cubic foam infilled TSP foldcore**	**Shaped foam infilled TSP foldcore**
Wall thickness (mm)	1.062	1.011	0.958
Mass of foam (g)	-	7.3	15.1
Mass of foldcore (g)	153.6	146.3	138.5
Density of core (kg/m^3)	150	150	150

Structural responses of the three claddings and the case with no cladding are listed in Table 7 and the transmitted force time-history curves are shown in Figure 17. Unlike in the previous section, the peak value of the transmitted force to the protected structure is very different for three configurations of claddings. The peak force is reduced by 50.8% for the cladding with TSP foldcore as compared to the unprotected case. For the two cases with foam infill, the peak transmitted force is reduced by 69.6% and 71.1% for the cubic and shaped foam filled foldcores, respectively. This difference in initial peak force is mainly caused by the variation of sidewall thickness. The cellular structure with thicker wall greatly increases the peak crushing force and greatly affects their crushing behaviours under dynamic loading due to the increasing inertia effect and the stabilization effect provided by the adjacent connecting faces [37].

Table 7. Peak transmitted force, peak crushed distance at centre and energy absorption by parts of different cladding configurations under 7 kg TNT explosion at 1.5 m stand-off distance

Cladding types	P_{peak} **(kN)**	**Peak crushed distance at centre δ (mm)**	**Energy absorption (J)**	
			by TSP foldcore	**by foam**
Without cladding	213.5	-	-	-
TSP foldcore	105.0	25.3	1328	-
Cubic foam filled	64.9	27.3	1253	32
Shaped foam filled	61.6	29.6	1241	98

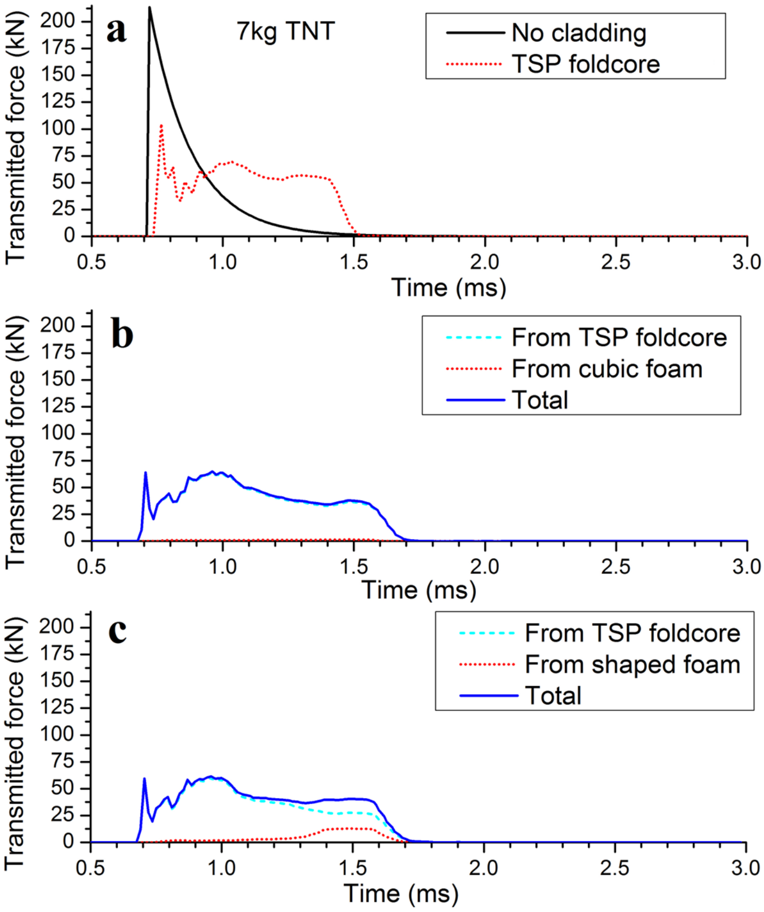

Figure 17. Computed time-history of transmitted forces to protected structure under 4kg TNT explosion at 1.5 m stand-off distance of four cladding configurations (a) no cladding and TSP foldcore without foam infill; (b) cubic foam filled TSP foldcore; (c) shaped foam filled TSP foldcore

Furthermore, a prolonged force-transmitting phase can be observed for the foam filled TSP foldcore as cladding. The force transmitting to the protected structure stops at around 1.5 ms for the cladding with TSP foldcore and 1.7 ms for the claddings with cubic and shaped foam filled TSP foldcore. The time-history curves of cubic foam and shaped foam infilled TSP foldcores are almost identical at the early stage of the loading (less than 1 ms). As explained previously, the deformation mode of the TSP foldcore under blast loading is different from that crushed under quasi-static loading. The top edges of the foldcore sidewalls bend towards unit cell centre under high loading rate, followed by the middle face buckling of the sidewalls. Therefore, the shaped foam infill provides little support to the sidewall at the early stage of the deformation under dynamic loading. However, slight crushing resistance increase is shown in the later stage of deformation (after 1.3 ms) for the shaped foam infilled TSP foldcore. This is caused by the support provided by the shaped foam to the buckled sidewalls, which is similar to the scenario shown in Figure 14 and Figure 15.

A great reduction in transmitted force is demonstrated for foam filled foldcores in this section (i.e. 7 kg TNT blast scenario). A further 41% reduction for shaped foam filled TSP foldcore is achieved comparing to the foldcore with foam infill. However, in the previous section (i.e. 1, 2, 4 kg TNT blast scenarios), the peak force reduction with three cladding configurations are similar. As higher overall core density is required for mitigation of higher blast loading (7 kg TNT blast), wall thickness increases for the case without foam infill which lead to increase in initial peak crushing resistance. This indicates that the foam infill is more effective than simply increasing the wall thickness of the foldcores to mitigate blast loading of higher intensity. In other words, to increase the blast mitigation capacity, the crushing resistance of cladding shall be increased which can be achieved by either thickening sidewall of foldcore or inserting lightweight foam. Foam insertion shows superior peak transmitted force reduction than using thicker wall of foldcore when experiencing higher intensity of blast loading.

5. Conclusion

The crushing behaviour under quasi-static loading condition and the blast mitigation capacity of foam filled TSP foldcore are examined in this study. Under quasi-static crushing, significant increase in crushing resistance of shaped foam filled TSP foldcore is observed. This is caused by the extra support provided by the foam to the foldcore sidewalls. Experimental results show that under quasi-static loading, the crushing resistance of shaped foam filled TSP foldcore is higher than the summation of two stand-alone components, indicating an effect of “1+1>2”. A numerical model is developed and verified against the quasi-static test. The calibrated numerical model is then used for the simulation of sacrificial cladding under various blast intensities. Significant reductions in peak transmitted force are observed for all claddings. The global damage may not be greatly reduced due to the mechanism of the sacrificial cladding [2, 32], as the total impulse transmitted on the protected structure is not greatly affected by the cladding configurations. The added cladding acts as a protective structure to reduce the local damage on the structure which is often caused by the high peak pressure in the event of blast.

Unlike quasi-static crushing test, both foam infilled (cubic and shaped) TSP foldcores show similar blast mitigation capability as the TSP foldcore without foam infill under lower blast intensities (i.e. 1, 2, 4 kg TNT). This is because of the change of the deformation mode under blast loading as compared to quasi-static crushing. The shaped foam provides little support to the sidewalls during the early bending of the top edges of foldcore towards the centre under blast loading. The crushing resistance has a slight rise at the later stage of the crushing due to compacting of the foam and the buckling at middle of sidewalls. It is also worth noting that under dynamic loading, shaped foam infill is more effective at the later stage of the foldcore deformation. The constraint provided to the TSP foldcore sidewalls by the shaped foam infill becomes active only when they are in contact with the foldcore at the later stage of deformation. Furthermore, the foldcore of higher density is studied under higher blast intensity (i.e. 7 kg TNT blast). It shows that both foam filled foldcores have much lower initial peak force transmitted to the protected structure as compared to the foldcore without foam infill, and the foam filled TSP foldcore experiences slightly larger peak centre displacement. Therefore, to withstand blast load of higher intensity, PU foam can be inserted inside the foldcore and it is more effective than simply increasing the wall thickness by yielding a much greater reduction in peak transmitted force to protected structure.

Acknowledgement

The authors acknowledge the support from Australian Research Council via Discovery Early Career Researcher Award (DE160101116).

Reference

[1] G.S. Langdon, D. Karagiozova, M.D. Theobald, G.N. Nurick, G. Lu, R.P. Merrett, Fracture of aluminium foam core sacrificial cladding subjected to air-blast loading, International Journal of Impact Engineering, 37 (2010) 638-651.

[2] A. Hanssen, L. Enstock, M. Langseth, Close-range blast loading of aluminium foam panels, International Journal of Impact Engineering, 27 (2002) 593-618.

[3] S. Guruprasad, A. Mukherjee, Layered sacrificial claddings under blast loading Part II—experimental studies, International Journal of Impact Engineering, 24 (2000) 975-984.

[4] H. Ousji, B. Belkassem, M.A. Louar, B. Reymen, J. Martino, D. Lecompte, L. Pyl, J. Vantomme, Air-blast response of sacrificial cladding using low density foams: Experimental and analytical approach, International Journal of Mechanical Sciences, 128-129 (2017) 459-474.

[5] C. Wu, L. Huang, D.J. Oehlers, Blast Testing of Aluminum Foam–Protected Reinforced Concrete Slabs, Journal of Performance of Constructed Facilities, 25 (2011) 464-474.

[6] L. Jing, Z. Wang, L. Zhao, Response of metallic cylindrical sandwich shells subjected to projectile impact—Experimental investigations, Composite Structures, 107 (2014) 36-47.

[7] S. Li, X. Li, Z. Wang, G. Wu, G. Lu, L. Zhao, Finite element analysis of sandwich panels with stepwise graded aluminum honeycomb cores under blast loading, Composites Part A: Applied Science and Manufacturing, 80 (2016) 1-12.

[8] L. Jing, Z. Wang, L. Zhao, The dynamic response of sandwich panels with cellular metal cores to localized impulsive loading, Composites Part B: Engineering, 94 (2016) 52-63.

[9] Z. Wang, H. Tian, Z. Lu, W. Zhou, High-speed axial impact of aluminum honeycomb – Experiments and simulations, Composites Part B: Engineering, 56 (2014) 1-8.

[10] C. Qi, A. Remennikov, L.-Z. Pei, S. Yang, Z.-H. Yu, T.D. Ngo, Impact and close-in blast response of auxetic honeycomb-cored sandwich panels: Experimental tests and numerical simulations, Composite Structures, 180 (2017) 161-178.

[11] S.C.K. Yuen, G. Nurick, The Use of Tubular Structures as Cores for Sandwich Panels Subjected to Dynamic and Blast Loading: A Current "State of the Art", in: Blast Mitigation, Springer, 2014, pp. 229-248.

[12] Z. Li, W. Chen, H. Hao, Numerical study of sandwich panel with a new bi-directional Load-Self-Cancelling (LSC) core under blast loading, Thin-Walled Structures, 127 (2018) 90-101.

[13] W. Chen, H. Hao, Numerical simulations of stiffened multi-arch double-layered panels subjected to blast loading, International Journal of Protective Structures, 4 (2013) 163-188.

[14] S. Heimbs, P. Middendorf, S. Kilchert, A.F. Johnson, M. Maier, Experimental and Numerical Analysis of Composite Folded Sandwich Core Structures Under Compression, Applied Composite Materials, 14 (2008) 363-377.

[15] X.M. Xiang, Z. You, G. Lu, Rectangular sandwich plates with Miura-ori folded core under quasi-static loadings, Composite Structures, 195 (2018) 359-374.

[16] K. Miura, Method of packaging and deployment of large membranes in space, The Institute of Space and Astronautical Science report, 618 (1985) 1.

[17] J.M. Gattas, Z. You, Quasi-static impact of indented foldcores, International Journal of Impact Engineering, 73 (2014) 15-29.

[18] R.K. Fathers, J.M. Gattas, Z. You, Quasi-static crushing of eggbox, cube, and modified cube foldcore sandwich structures, International Journal of Mechanical Sciences, 101-102 (2015) 421-428.

[19] Z. Li, W. Chen, H. Hao, Crushing behaviours of folded kirigami structure with square dome shape, International Journal of Impact Engineering, 115 (2018) 94-105.

[20] Z. Li, W. Chen, H. Hao, Blast mitigation performance of cladding using Square Dome-shape Kirigami folded structure as core, International Journal of Mechanical Sciences, 145 (2018) 83-95.

[21] Z. Li, W. Chen, H. Hao, Blast resistant performance of cladding with folded open-top truncated pyramid structures as core, in: 7th International Meeting on Origami in Science, Mathematics, and Education, Oxford, UK, 2018.

[22] G. Zhang, B. Wang, L. Ma, L. Wu, S. Pan, J. Yang, Energy absorption and low velocity impact response of polyurethane foam filled pyramidal lattice core sandwich panels, Composite Structures, 108 (2014) 304-310.

[23] P.J. Tan, J.J. Harrigan, S.R. Reid, Inertia effects in uniaxial dynamic compression of a closed cell aluminium alloy foam, Materials science and technology, 18 (2002) 480-488.

[24] T. Nieh, K. Higashi, J. Wadsworth, Effect of cell morphology on the compressive properties of open-cell aluminum foams, Materials Science and Engineering: A, 283 (2000) 105-110.

[25] ASTM, E8M-04 Standard Test Methods for Tension Testing of Metallic Materials (Metric) 1, ASTM international, 2004.

[26] Z. Li, W. Chen, H. Hao, Numerical study of open-top truncated pyramid folded structures with interconnected side walls against flatwise crushing, Thin-Walled Structures, 132 (2018) 537-548.

[27] S. Hou, X. Han, G. Sun, S. Long, W. Li, X. Yang, Q. Li, Multiobjective optimization for tapered circular tubes, Thin-Walled Structures, 49 (2011) 855-863.

[28] Y. Zhang, X. Xu, G. Sun, X. Lai, Q. Li, Nondeterministic optimization of tapered sandwich column for crashworthiness, Thin-Walled Structures, 122 (2018) 193-207.

[29] W. Chen, T. Wierzbicki, Relative merits of single-cell, multi-cell and foam-filled thin-walled structures in energy absorption, Thin-Walled Structures, 39 (2001) 287-306.

[30] G. Sun, S. Li, Q. Liu, G. Li, Q. Li, Experimental study on crashworthiness of empty/aluminum foam/honeycomb-filled CFRP tubes, Composite Structures, 152 (2016) 969-993.

[31] Z. Wang, J. Liu, Z. Lu, D. Hui, Mechanical behavior of composited structure filled with tandem honeycombs, Composites Part B: Engineering, 114 (2017) 128-138.

[32] G.W. Ma, Z.Q. Ye, Analysis of foam claddings for blast alleviation, International Journal of Impact Engineering, 34 (2005) 60-70.

[33] CYMAT, Technical Manual for CYMAT SmartMetal™, CYMAT Technologies Ltd, (2009) 5-1-17.

[34] F. Zhu, L. Zhao, G. Lu, Z. Wang, Structural response and energy absorption of sandwich panels with an aluminium foam core under blast loading, Advances in Structural Engineering, 11 (2008) 525-536.

[35] S. Ouellet, D. Cronin, M. Worswick, Compressive response of polymeric foams under quasi-static, medium and high strain rate conditions, Polymer Testing, 25 (2006) 731-743.

[36] J. Zhang, M. Ashby, The out-of-plane properties of honeycombs, International Journal of Mechanical Sciences, 34 (1992) 475-489.

[37] Z. Xue, J.W. Hutchinson, Crush dynamics of square honeycomb sandwich cores, International Journal for Numerical Methods in Engineering, 65 (2006) 2221-2245.